

Eddy Current Detection of the Martensitic Transformation in AISI304 Induced upon Cryogenic Cutting

Lara V. Fricke,* Hai Nam Nguyen, Bernd Breidenstein, David Zaremba,* and Hans Jürgen Maier

The combination of a hard subsurface layer and a ductile component core is advantageous for many applications. Steels are often heat treated to create such a hardened subsurface, which is both time- and energy-consuming. It is of great advantage to create a hardened subsurface directly within the machining process, as the production line of most components includes such a process to produce the desired geometric dimensions and surface quality. To achieve a martensitic subsurface layer within the machining process, cryogenic, external turning using a metastable AISI304 austenitic steel is used herein. Herein eddy current testing and the analysis of higher harmonics are used for the detection of the ferromagnetic, martensitic phase in the parent austenite. A good correlation is found between the martensite content and the amplitude of the signals measured. Therefore, eddy current testing is considered as a suitable real-time, nondestructive testing method, which forms the basis for the generation of a tailored, deformation-induced martensitic subsurface layer during external turning.

benefit if no additional heat treatment process would be required to create a hardened subsurface.

Deep rolling is used for strain-induced martensitic transformation in the near-surface layer, so that surface hardening can be achieved without heat treatment process within the production line.^[1] Cryogenic deep rolling of metastable austenites is an approach to achieve an even better martensitic surface hardening of steel components in a heat treatment-free production line.^[2] The lower the deformation temperature, the more martensite can be formed. This is due to the strong dependence of the deformation-induced martensitic transformation (DIMIT) on the stacking fault energy (SFE) of the alloy.^[3] The SFE depends on many factors,^[4] e.g., alloy composition, grain size, stress state, initial

1. Introduction


In addition to high ductility, a hard subsurface layer is of great importance for components to withstand high mechanical and tribological loads. Typically, an appropriate microstructure is generated via heat treatment processes in the near-surface region. However, these processes are time- and energy-consuming and can result in component distortion. Therefore, it would be of great

texture, and temperature.^[5,6] In general, low SFE alloys, such as metastable stainless steels, show martensitic transformations^[3] and lower the temperature, lower the SFE, and the more pronounced the DIMIT.^[6,7] The DIMIT can be triggered below the so-called M_d temperature.^[8,9] Shin et al. described that less stress is needed to induce martensitic transformation with decreasing temperature,^[9] and once the M_s temperature is reached martensitic transformation will take place without superimposed external stress. These two characteristic temperatures depend on the alloy composition and for metastable austenitic steels they can be calculated using the equations suggested by Angel^[10] for the M_{d30} temperature, where 50% of martensite is formed after a true strain of 30%, and by Eichelman and Hull^[11] for the M_s temperature.

In comparison with deep rolling, it would be of even greater use to create a martensitic subsurface layer by machining, e.g., by an external turning process, as such processes are integrated in almost every production line. Machining typical results in a strain rate between 10^3 and 10^6 s^{-1} .^[12] However, DIMIT is curtailed when the strain rate increases, mainly due to the increase in adiabatic heat.^[6] Strain rates up to 10^3 s^{-1} lead to an increase in yield strength but also to a reduction in work hardening due to adiabatic heating of the specimen.^[13,14] Cao et al. found as well that with strain rates, up to 10^3 s^{-1} , the temperature changes increase compared with quasistatic tensile tests. On the other hand, the maximum martensitic volume fraction is less than one-fifth for strain rates over 10^3 s^{-1} than for quasistatic strain rates ($< 0.2 \text{ s}^{-1}$).^[14] For strain rates above 10^5 s^{-1} , Eckner et al. observed the formation of stacking faults, shear bands, and deformation-induced

L. V. Fricke, Dr. D. Zaremba, Prof. H. J. Maier
Institut für Werkstoffkunde
Leibniz Universität Hannover
An der Universität 2, 30823 Garbsen, Germany
E-mail: fricke@iw.uni-hannover.de; zaremba@iw.uni-hannover.de

H. N. Nguyen, Prof. B. Breidenstein
Institut für Fertigungstechnik und Werkzeugmaschinen
Leibniz Universität Hannover
An der Universität 2, 30823 Garbsen, Germany

 The ORCID identification number(s) for the author(s) of this article can be found under <https://doi.org/10.1002/srin.202000299>.

© 2020 The Authors. Steel Research International published by Wiley-VCH GmbH. This is an open access article under the terms of the Creative Commons Attribution-NonCommercial-NoDerivs License, which permits use and distribution in any medium, provided the original work is properly cited, the use is non-commercial and no modifications or adaptations are made.

The copyright line for this article was changed on 12 March 2021 after original online publication.

DOI: 10.1002/srin.202000299

martensite,^[15] and Hecker et al. found that the temperature increase due to adiabatic heating was sufficient to suppress the martensitic transformation at high strain rates.^[16] Consequently, the temperature in the zone ahead of the tool tip should be kept low, and thus cryogenic, external turning was used in the present study to promote martensitic transformation.

Nondestructive testing methods for quality control are key to ensure a defined, production-integrated martensitic subsurface hardening. Various studies^[14,17–22] have already monitored martensite formation upon plastic deformation of stainless steels with magnetic testing methods. However, most nondestructive, magnetic testing methods can lead to a misjudgment of martensite fraction due to inhomogeneous martensite distribution over the thickness.^[23] One way to determine the DIMT behavior of steel is the nondestructive determination of the relative magnetic permeability by eliminating the influence of the jigs, which was done by Cao et al. using DC voltage instead of AC voltage.^[14,19] Another possibility to achieve more accurate results is to use eddy current testing as the excitation frequency can be varied and different studies demonstrate a good correlation between the martensite content and measured values in eddy current testing. For example, Silva et al. showed an exponential correlation between martensite volume fraction and phase angle^[4] and Khan et al. between coil impedance, impedance phase, and martensite content.^[22] Compared with the method developed by Cao et al.,^[19] which was designed for tensile samples, it is already known in many ways that eddy current sensors can be integrated into production processes.^[24,25]

To be able to perform defined, production-integrated subsurface hardening, the influence of two cutting parameters, namely temperature and feed, on the DIMT was analyzed in the present study. The martensite content was determined using eddy current technology. The experimental details are given

in Section 4. Based on the findings of earlier work conducted by Mroz et al., according to which the third harmonic of the eddy current signal is most suited for the determination of magnetic material properties, it was expected that this characteristic value is best applicable for the determination of martensite content.^[26]

2. Results and Discussion

2.1. Influence of the Cutting Parameters on Phase Transformation and Residual Stresses

Figure 1, 2 show the results of the X-ray diffraction (XRD) measurements. The maximum fraction of α' martensite was determined to be present at a depth of approximately 18 μm . On the one hand, the phase transformation at the surface is less pronounced than slightly below the surface due to a higher local temperature.^[27] For the same reason, when looking at the residual stress in axial direction, it can be seen that there are tensile residual stresses at the surface, as no lubricant was used during turning. There are lubricants that can be used down to $-30\text{ }^\circ\text{C}$.^[28] However, in the present study, experiments at significantly lower temperatures were conducted, and thus lubricants were avoided throughout. As the distance to the surface increases, the effect of phase transformation starts to dominate, and there are compressive residual stresses in the microstructure, see Figure 2. Different from the effect on martensite volume fraction, the test temperature does not significantly influence the formation of residual stress. In contrast, the feed has an obvious effect on the residual stress formation, and the stress–depth profile is shifted toward more positive stress values with higher feeds, see Figure 2. This is an indication that locally a higher

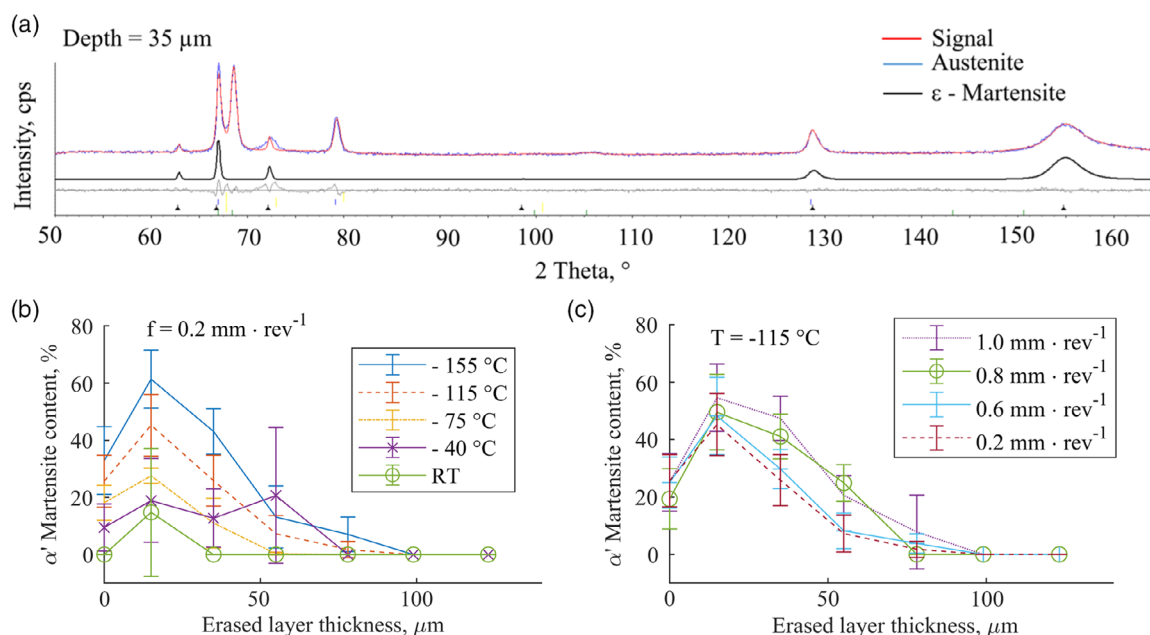


Figure 1. XRD results demonstrating a) the presence of ϵ martensite and the change in α' content with distance to surface as function of b) temperature and c) feed.

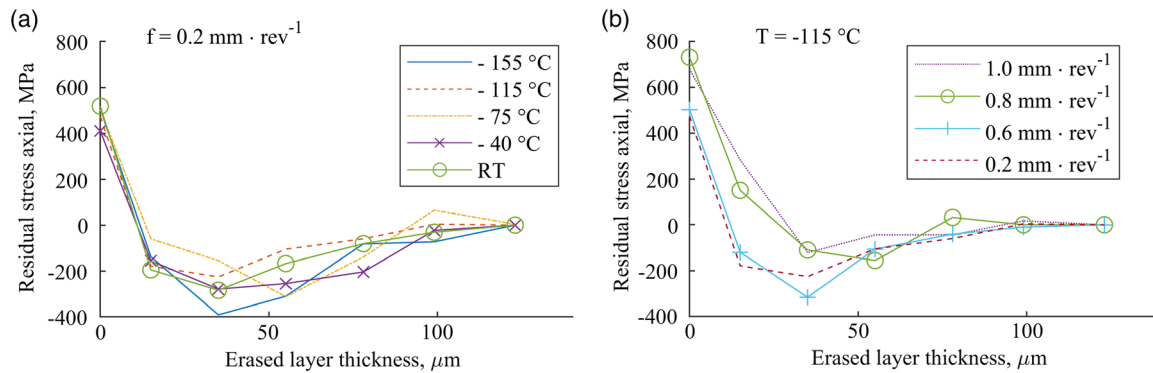


Figure 2. XRD results for axial residual stress as a function of surface distance for different cutting a) temperatures and b) feeds.

temperature was induced at higher feeds. Further, it is shown that the lower the temperature and the higher the feed was, the more the α' martensite is formed. To make sure that the transformation was not due to just lowering the temperature, a reference sample was cooled down to $-150\text{ }^\circ\text{C}$ but was not machined. As expected, no martensite was formed in this case.

A lower temperature results in a lower SFE and a higher feed results in higher cutting forces, and thus DIMT is promoted.^[27,29] From Figure 1, it is also clear that lowering the temperature is more effective to create a higher martensite content than increasing the feed. This can be attributed to the increase in local temperature that accompanies an increase in cutting force. This in turn leads to a higher SFE and therefore, more energy is needed to trigger the DIMT.

Nevertheless, with increasing feed, the martensite content still increases. This is in accordance with results obtained by Mayer et al.,^[27,29] who found that the high mechanical load overcompensates the increase in temperature.^[29] In Figure 1, it is shown that maximum martensite content for all feeds is similar. However, the content for higher feeds is increased at a greater depth. This can be attributed to the higher forces that are caused by increasing the feed, albeit, closer to the surface, higher work temperatures seem to compensate the higher forces regarding the phase transformation.

In addition, a second phase was detected by XRD in all samples. This phase has its maximum content at a surface distance of about $35\text{ }\mu\text{m}$, where the maximum magnitude of the compressive stress is found. The phase was determined to be ϵ martensite, using the hexagonal lattice parameters $a_{\epsilon(\text{hcp})} = 2.548\text{ }\text{\AA}$ and $c_{\epsilon(\text{hcp})} = 4.162\text{ }\text{\AA}$.^[30] It is reported that α' martensite is more likely to form on intersections of ϵ martensite.^[31,32] Furthermore, Schumann found that steels having SFE lower than $20\text{ mJ} \cdot \text{m}^{-2}$ transform via the $\gamma \rightarrow \epsilon \rightarrow \alpha'$ mechanism, which is the case for AISI304.^[33] Celada-Casero et al. found that if a strain over 0.2 is reached, ϵ martensite can be detected.^[20] It should be noted that ϵ martensite is paramagnetic and cannot be detected using the third harmonic of the eddy current signal. Thus, a combination of XRD and eddy current testing is needed to shed light on the underlying mechanisms and be able to rapidly probe phase transformation upon machining.

Comparing the cutting parameters, it is shown that the starting temperature of the workpiece and the feed have the most

dominant effect on DIMT. Thus, the highest amount of martensite can be produced at the lowest possible temperature and the highest feed. However, the higher the feed, the rougher the surface will be and therefore, the increase in feed is limited with respect to the desired surface quality of the component.

2.2. Characteristics of the Martensitic Phase Transformation at Low Temperature and High Cutting Forces

Figure 3 shows metallographic cross sections of four samples turned at $-40\text{ }^\circ\text{C}$ and $-115\text{ }^\circ\text{C}$ at a feed of $0.2\text{ mm} \cdot \text{rev}^{-1}$ and at $-115\text{ }^\circ\text{C}$ $0.8\text{ mm} \cdot \text{rev}^{-1}$ and $1.0\text{ mm} \cdot \text{rev}^{-1}$. The areas that appear black can in principle be martensite, twins, and deformation lines. These are difficult to distinguish under the light microscope, which is why additional scanning electron microscopy (SEM) pictures were taken. Figure 4 shows that there is martensite, deformation-induced twins, and deformation lines, as well as thermal twins in the subsurface zone. Further, an influence of the cutting feed on the deformation behavior was detected. At $0.2\text{ mm} \cdot \text{rev}^{-1}$, Figure 3a,b, one can see deformation bands and deformation-induced twins, mostly in one plane of the plane family $\{111\}$. As the feed rate increases, fewer deformation bands can be found and more twins are formed. In addition, more twins in the second plane of the plane family $\{111\}$ can be found. It seems that the stress with increasing depth has a greater influence on the deformation than strain, which causes the martensitic transformation. Moreover, deformation takes place at a greater depth with a smaller feed rate. In Figure 3c,d, no deformation lines can be found in the martensitic subsurface layer. In Figure 3a,b, however, deformation lines can be seen underneath the martensitic subsurface layer.

Further, in Figure 3, it is shown that the black-appearing areas increase with decreasing temperature and increasing feed. This demonstrates an increase in martensite content, which was verified by the XRD results as well by the hardness measurements carried out, where three hardness values were taken at a depth of $\approx 60\text{ }\mu\text{m}$. The hardness values of the martensitic subsurface zones are shown in the upper right corner in Figure 3. The hardness of the undeformed material was $169 \pm 13\text{ HV}0.1$, so martensitic transformation led to significant hardness increase.

In the SEM images, many parallel lines were seen in all samples, which indicate lath martensite.^[31–33] Lath martensite

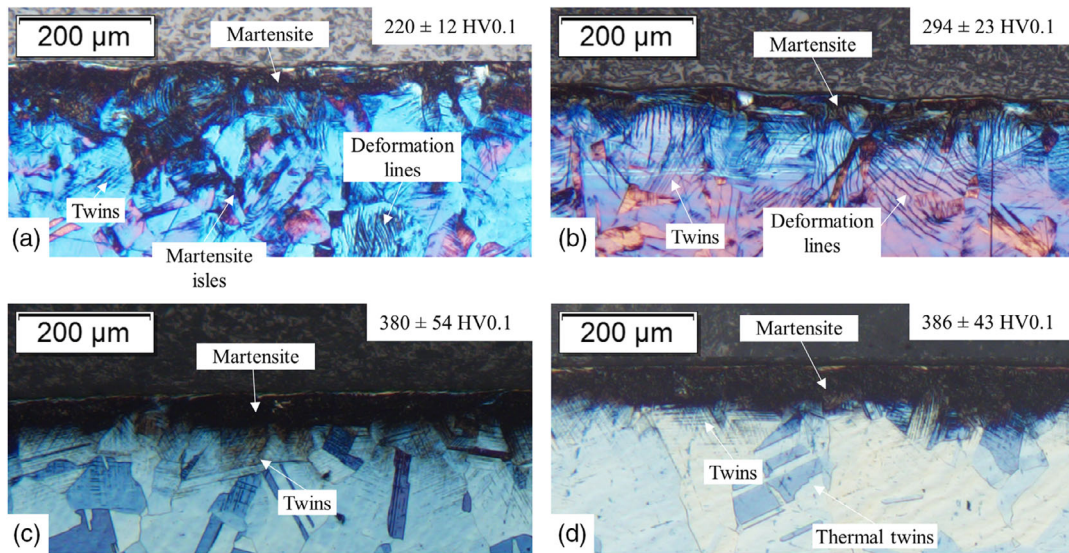


Figure 3. Metallographic cross sections for a feed of $0.2 \text{ mm} \cdot \text{rev}^{-1}$ at a temperature of a) $-40 \text{ }^\circ\text{C}$, b) $-115 \text{ }^\circ\text{C}$ and at a temperature of $-115 \text{ }^\circ\text{C}$ for a feed of c) $0.8 \text{ mm} \cdot \text{rev}^{-1}$ and d) $1.0 \text{ mm} \cdot \text{rev}^{-1}$.

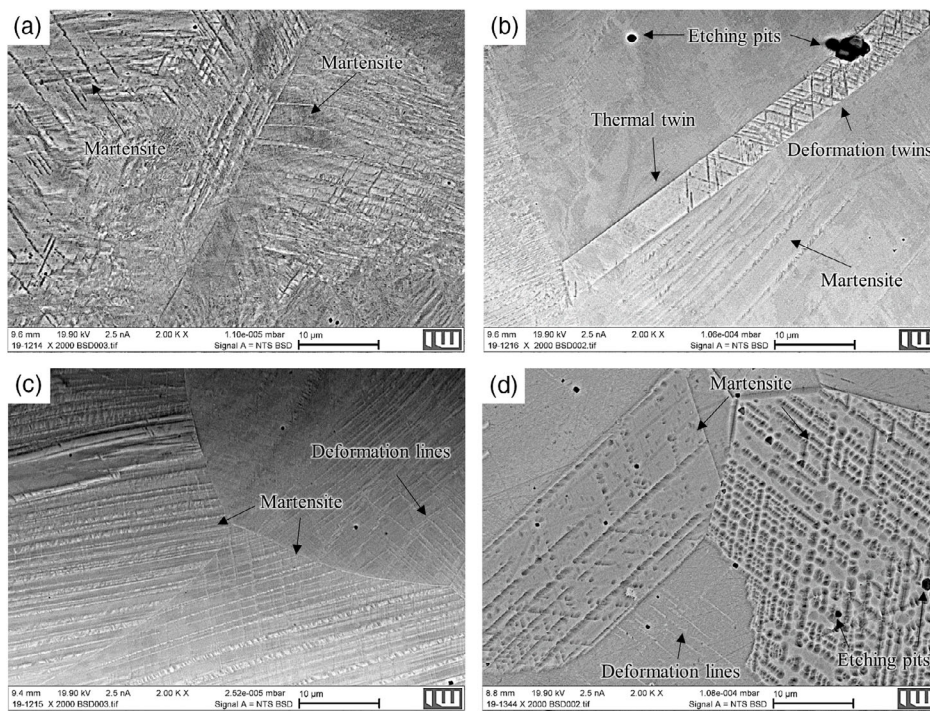


Figure 4. SEM pictures for cutting temperature variation for a feed of $0.2 \text{ mm} \cdot \text{rev}^{-1}$: a) $-40 \text{ }^\circ\text{C}$ and b) $-75 \text{ }^\circ\text{C}$ and feed variation at a temperature of $-115 \text{ }^\circ\text{C}$: c) $0.2 \text{ mm} \cdot \text{rev}^{-1}$ and d) $0.8 \text{ mm} \cdot \text{rev}^{-1}$.

is produced by strain-induced martensitic transformation,^[31,34] i.e., the samples experienced a higher stress than the yield stress of the austenitic phase. According to Weiß et al. stress-induced martensite is possible to occur for AISI304 for temperatures lower than $-60 \text{ }^\circ\text{C}$ if the applied stress level is below the yielding point.^[35] In this case, the martensite is plate shaped. As no plate-shaped martensite could be detected in the present

study, this is another indication that the locally applied stress is above the yield stress of the austenite.

Mayer et al. conducted their study using similar cutting parameters. They measured the cutting forces and determined the equivalent stress distribution in the workpiece.^[27] The equivalent stress induced by machining is, for the parameters used here, more than ten times higher than the yield strength of AISI304

(≈ 300 MPa at -115 °C^[35]). This also fits with the observation that no plate-shaped martensite was found in the present study. However, a major disadvantage of the calculation of equivalent stress distribution is that the Hertzian stress is normally used,^[27] and therefore no plastic deformation is considered.

By lowering the temperature, the strength of the austenitic materials increases so that more force is required to produce the desired depth of the cut,^[27] which was kept constant for all samples produced in the present study. Further, the development of a built-up edge with decreasing temperature can be observed in face-centered cubic materials.^[27] Hence, a higher force is required to continue the turning process. Thus, a higher force is applied with decreasing component temperature, which in turn promotes strain-induced martensite transformation. In addition, the energy required for strain-induced martensite transformation becomes lower the closer the temperature gets to M_s , as well as more dislocations are formed which enhances conditions which support a strain-induced transformation. That might be why there is still no stress-assisted martensite even though the temperature is low enough.

As the material properties depend on the microstructure, there is a difference between samples containing lath or plate martensite.^[36–38] Thus, knowing which combination of cutting parameters produces which type of martensite appears to be useful to create a subsurface zone with specific or tailored mechanical properties by a controlled turning process.

2.3. Correlation Between Eddy Current Measurement Signals and Martensitic Transformation

In **Figure 5** the clear correlation between the amplitude of the third harmonic of the eddy current signal and the cutting parameters is shown. This is expected, as the amplitude of the third harmonic increases with increasing content of α' martensite, and the latter depends on feed and temperature, see **Figure 1**. As the amplitude of the third harmonic is a reliable parameter to detect α' martensitic transformation, it appears that eddy current testing could be a viable nondestructive tool for the

implementation of an in-line measurement system in a cutting machine.

Furthermore, it can be seen that the amplitude of the third harmonic takes on higher values by increasing the feed. The maximum martensite content was found by XRD for the turning parameters -155 °C and 0.2 mm \cdot rev⁻¹. However, the maximum amplitude of the third harmonic was found for the parameters -115 °C and 0.8 mm \cdot rev⁻¹. Moreover, the standard deviation for the samples where the temperature was varied is very small compared with the standard deviations of the samples where the feed was varied. For the high feed, the surfaces appeared thread like (R_a between 15 and 8 μ m, R_z between 55 and 29 μ m). The distribution of eddy currents is influenced by sharp edges that are present in the thread-like surface, which leads to a higher secondary field. This in turn causes a higher apparent martensite content. Consequently, the third harmonic will only reflect martensite content accurately for samples that have a good surface quality. Despite this roughness-induced artefact, the eddy current technology can still be considered a useful tool to detect the martensite content of turned shafts, as low surface roughness is a requirement for high-performance components.

An additional correlation is shown between the martensitic content and the phase of the first harmonic, as shown in **Figure 6a,b**. With increasing martensite content, the phase decreases. It is advantageous if more than one parameter can be correlated with the desired measurement value especially, when using an electromagnetic nondestructive testing method where a one-to-one correlation is not possible because the magnetic and electrical properties of the subsurface are not only influenced by the martensite content but also by other factors such as residual stresses, dislocation density, and grain size.

The phase of the first harmonic seems to respond more sensitively to the deformed austenite. The deformation of the austenite is not visible in the third harmonic because the paramagnetic austenite does not change the waveform of the measurement signal. Workpiece temperature has a pronounced effect on phase, and the sample machined at -155 °C shows the lowest phase, see **Figure 6**. Looking at **Figure 3a,b** more deformation lines are shown in **Figure 3b**, where a lower

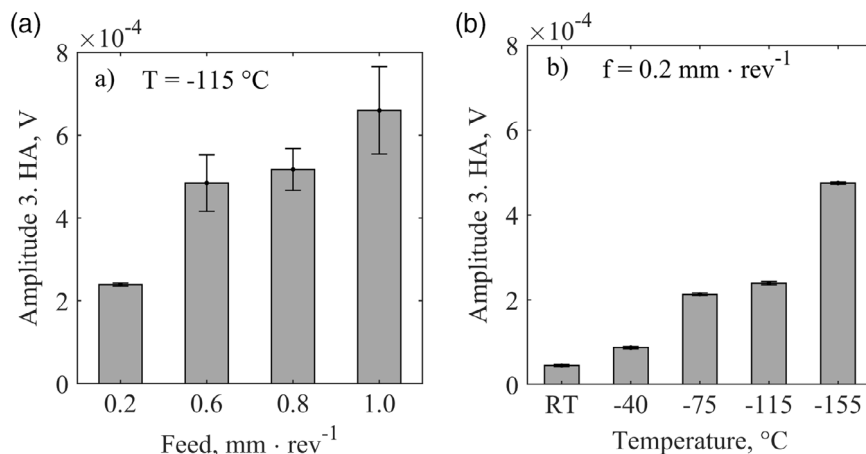


Figure 5. Determination of the ferromagnetic α' martensitic content using the amplitude of the third harmonic of the eddy current signal for the variation of a) feed and b) temperature; the average values of five measurements are shown and error bars indicate standard deviation.

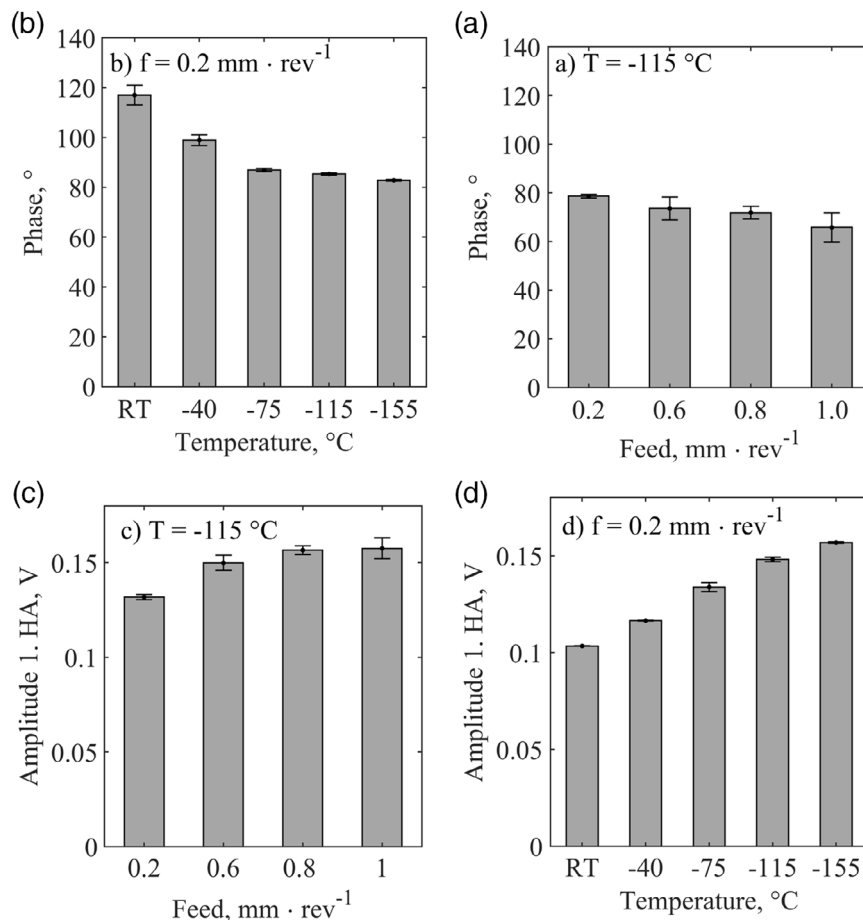


Figure 6. Determination of the austenite deformation using the phase and amplitude of the first harmonic of the eddy current signal for different a) + c) feeds and b) + d) temperatures; the average values of five measurements are displayed along with their standard deviation.

workpiece temperature was applied. Here, an increase in deformation lines in the austenite can be seen the lower the workpiece temperature. Comparing Figure 3c,d, it is shown that the amount of deformation lines is similar. Therefore, the phase change of the first harmonic is smaller compared with the changes due to the temperature decrease. Nevertheless, in another study, it was found that the phase of the first harmonic is more pronounced to the influence of the eddy current sensor–workpiece distance.^[39] Hence, if there are any changes in geometrical arrangement, it might lead to a misinterpretation of the martensite content. Therefore, it would be preferable to use another parameter to detect the martensite content.

A further correlation can be seen between the martensitic content and the amplitude of the first harmonic, as shown in Figure 6c,d. With increasing martensite content, the amplitude increases. This is in good correlation with the electrical and magnetic properties that influence the first harmonic. The martensitic phase is electrically more conductive than the parent austenite and ferromagnetic; therefore, the amplitude of the first harmonic increases. Further, the standard deviation is smaller compared with the third harmonic. Hence, the first harmonic seems to be less influenced by disturbances than the third harmonic in this case.

It is advantageous if more than one parameter can be correlated with the desired measurement value especially, when using an electromagnetic nondestructive testing method where a one-to-one correlation is not possible because the magnetic and electrical properties of the subsurface are not only influenced by the martensite content but also by other factors such as residual stresses, dislocation density, and grain size. Thus, both the amplitude of the third harmonic and the amplitude of the first harmonic correlate with the changes in the material due to the deformation and in combination they offer the best potential to detect those changes.

3. Conclusion

Although DIMT is suppressed at high strain rates, the present study shows that it is possible to induce a DIMT by cryogenic machining using AISI304, which is a widely used metastable stainless steel. The data obtained demonstrate that there two counteracting mechanisms during turning that govern the amount of martensite formation. The lower the temperature, the more the martensite can be induced, and the resulting higher cutting forces also promote martensite formation. However,

the higher the cutting forces, the higher the local temperature, and thus the higher the SFE. This in turn leads to a decrease in martensitic phase transformation. Therefore, a reduction of the cutting temperature seems to be the most suitable method to increase martensite content induced by DIMT due to machining.

The use of eddy current testing with higher harmonics analysis is a powerful nondestructive tool to evaluate martensitic content. Specifically, a good correlation was found between the amplitude of the third and the phase of the first harmonic and martensite content. Hence, this nondestructive testing method appears as a viable approach to realize automatic control in a cutting machine for setting a desired amount of martensite in a subsurface layer and thus tailor this zone during the machining process.

4. Experimental Section

Materials, Machining, and Methods: The experiments were conducted using an AISI304 metastable austenitic steel, which was solution annealed at 1050 °C for 45 min and slowly cooled in argon atmosphere by turning the oven off to obtain a homogeneous microstructure.

The measured alloying composition was 0.028 wt% C, 0.492 wt% Si, 1.90 wt% Mn, 18.24 wt% Cr, 0.406 wt% Mo, 7.95 wt% Ni, and 0.093 wt% N and Fe balance. Using this composition, the M_d and M_s temperature was calculated according to the following equations^[10,11]

$$M_{d30}(\text{°C}) = 413 - 462[(C + N)] - 9.2[\text{Si}] - 8.1[\text{Mn}] - 13.7[\text{Cr}] - 9.5[\text{Ni}] - 18.5[\text{Mo}] \quad (1)$$

$$M_s(\text{°C}) = 75(14.6 - [\text{Cr}]) + 110(8.9 - [\text{Ni}]) + 60(1.33 - [\text{Mn}]) + 50(0.47 - [\text{Si}]) + 3000(0.068 - [C + N]) \quad (2)$$

M_d and M_s were calculated to be close to 273 K and 0 K, respectively. Therefore, it can be expected that a transformation of austenite in martensite will occur by applying stress but not by only decreasing the temperature.

Machining was conducted with an external turning process using different workpiece temperatures and feeds to analyze their influence. In **Table 1** the cutting parameters are shown. When the temperature was varied, the feed amounted 0.2 mm. The temperature was set between -155 °C and room temperatures and was adjusted using liquid nitrogen. The temperature steps are shown in Table 1. The samples were placed in a container filled with liquid nitrogen for a certain time until the desired temperature was reached. The temperature was measured using a thermocouple type K in a borehole in the core of the samples directly before placing the samples in the lathe. No further cooling or lubricant was applied during cutting. After cutting, the temperatures were about 10 °C higher than before cutting. The cutting speed was set at 150 m · min⁻¹, the cutting depth was 0.2 mm, the tool orthogonal rake angle was constant at -6° and an unworn cutting edge with an average cutting edge rounding of 10 μm was used. The feed was varied between 0.2 mm · rev⁻¹ and 1 mm · rev⁻¹ at a temperature of -115 °C. The different feeds are shown in Table 1.

Table 1. Cutting parameters varied.

Cutting speed [[m] [min] ⁻¹]	Feed [mm · rev ⁻¹]	Cutting depth [mm]	Temperature at beginning [°C]	Cutting edge radius [μm]	Depth of martensite transformation [μm]
150	0.6, 0.8, 1.0	0.2	-115	10	99, 78, 96
150	0.2	0.2	RT, -40, -75, -115, -155	10	17, 54, 56, 79, 101

Microstructural and Phase Analyses: For optical microscopy the samples were polished using as little force as possible (25–30 N). The samples were ground with 1200 grit SiC paper and then polished with 3 μm particles. The color etchant Braha II was applied after polishing the samples, and images were taken with Leica, DM4000M microscope. For in-depth microstructural analysis, a scanning electron microscope (Zeiss Supra 55VP) was used and the samples were etched using a V2A stain.

Phase analyses and residual stress measurements in axial direction were carried out by XRD with Cr K α radiation using a dual-circuit diffractometer system XRD 3003 TT. The martensite content was obtained by a heuristic method developed by G. Faninger and U. Hartmann.^[40] Here the mean values of the ratios of the intensities of martensite and austenite of different crystallographic planes were determined. From this, the martensite content for each ratio of the crystallographic planes was derived. The mean value was then calculated over all crystallographic planes. The turning process created a texture within the samples, which explained the standard deviations, as shown in Figure 2. To obtain the desired information as a function of distance to the sample surface, several micrometers were erased by etching, before new measurements were carried out. This is the value shown on the x-coordinate in Figure 1,2.

Eddy Current Testing and Analysis of Higher Harmonics: **Figure 7** shows the principles of eddy current testing and the analysis of higher harmonics. An excitation coil generated an alternating magnetic field, which induced eddy currents in an electrically conductive material. An excitation frequency of 6.4 kHz was used here. Due to the skin effect, the penetration depth of eddy currents depends, among others, on excitation frequency. The higher the frequency, the smaller the penetration depth and hence, the influence of the subsurface on the measurement results is more pronounced. It was found that 6.4 kHz is high enough to see the martensitic transformation and mostly gain information from the subsurface. In addition, the penetration depth was still sufficient to distinguish samples with greater deformation depths and therefore, the chosen frequency was not too high, so the entire transformation was taken into account. Further, the formation of eddy currents depends on the magnetic and electrical material properties. Those eddy currents created an opposing secondary magnetic field, which overlapped with the primary magnetic field. The resulting magnetic field induced a voltage in the measuring coil, which was measured and demodulated. This is called harmonic analysis of eddy current signals and is often used for material characterization and for the nondestructive determination of mechanical properties.^[41]

In the paramagnetic material state, the relative magnetic permeability μ_r has a constant value, so that there is a linear relationship between the magnetic field strength and the flux density. A sinusoidal excitation current therefore leads to an undistorted sinusoidal measurement voltage. The measurement signal demodulated by fast Fourier transformation (FFT) contains only the test or fundamental frequency, first harmonic, and does not show any higher harmonic signal components in its spectrum. In the ferromagnetic state, there is a nonlinear relationship between the magnetic field strength and the magnetic flux density, which is also characterized by the magnetic hysteresis curve as transfer function and leads to a distorted measurement signal and odd-numbered multiples of the test frequency (e.g., the third harmonic and fifth harmonic) in the measurement signal in addition to the first harmonic. After demodulation of the measurement signal, the fundamental frequency and the higher harmonic signal components can be evaluated separately with regard to their amplitude and phase.^[26,42–44] As in conventional eddy current testing, the first harmonic provides information on the electrical and magnetic material

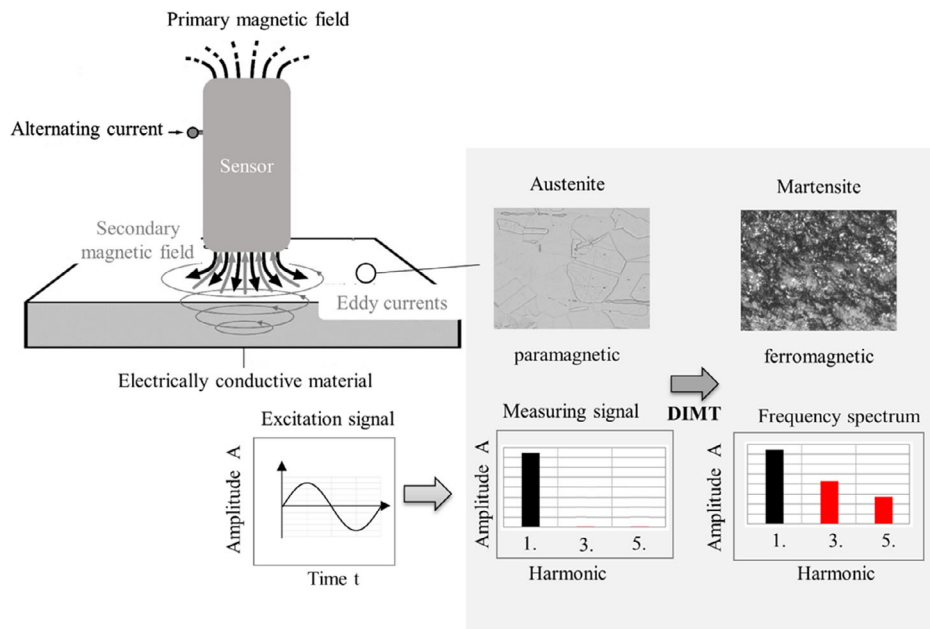


Figure 7. Schematic illustrating eddy current testing with analysis of the higher harmonics that are caused by deformation-induced martensite transformation.

properties. In contrast, the higher harmonics in the measurement signal, which are directly related to the shape and characteristics of the magnetic hysteresis curve, provide information that is mainly influenced by the magnetic material properties.^[26,42]

For example, the analysis of higher harmonics can be used to differentiate decarburizing depth due to a change in the magnetic properties of the steels^[43] as well as the carburizing depth due to the content of retained austenite within the subsurface.^[44] In this study it allows a differentiation between paramagnetic austenite and ferromagnetic martensite newly formed by DIMT. The newly formed, ferromagnetic martensite generates higher harmonics and also influences the first harmonic.

Acknowledgements

The scientific work was supported by the DFG within the research priority program SPP 2086 (grant project no. 401800578). The authors thank the DFG for this funding and intensive technical support. In addition, the authors thanks Lia Jablonik for preparing and analyzing metallographic samples and Lorenz Gerdes for conducting the XRD measurements.

Conflict of Interest

The authors declare no conflict of interest.

Keywords

deformation-induced martensites, eddy current testings, harmonic analyses, machining, metastable austenitic steels

Received: May 26, 2020

Revised: October 9, 2020

Published online: October 25, 2020

- [1] E. Brinksmeier, M. Garbrecht, D. Meyer, J. Dong, *Prod. Eng. Res. Devel.* **2008**, 2, 109.
- [2] D. Meyer, E. Brinksmeier, F. Hoffmann, *Proc. Eng.* **2011**, 19, 258.
- [3] M. Moallemi, A. Kermanpur, A. Najafzadeh, A. Rezaee, H. S. Baghbadorani, P. D. Nezhadfar, *Mater. Sci. Eng. A* **2016**, 653, 147.
- [4] V. M. A. Silva, C. G. Camerini, J. M. Pardal, J. C. G. de Blás, G. R. Pereira, *J Mater Res Technol.* **2018**, 7, 395.
- [5] M. H. Cai, W. J. Zhu, N. Stanford, L. B. Pan, Q. Chao, P. D. Hodgson, *Mater. Sci. Eng. A* **2016**, 653, 35.
- [6] A. Das, S. Tarafder, P. C. Chakraborti, *Mater. Sci. Eng. A* **2011**, 529, 9.
- [7] P. M. Ahmedabadi, V. Kain, A. Agrawal, *Mater. Des.* **2016**, 109, 466.
- [8] A. Kovalev, A. Jahn, A. Weiß, P. R. Scheller, *Steel Res. Int.* **2011**, 82, 45.
- [9] H. C. Shin, T. K. Ha, Y. W. Chang, *Scr. Mater.* **2001**, 45, 823.
- [10] T. Angel, *J. Iron Steel Inst.* **1954**, 177, 165.
- [11] G. H. Eichelman, F. C. Hull, *Trans. ASM* **1952**, 45, 77.
- [12] S. P. F. C. Jaspers, *Metal Cutting Mechanics And Material Behaviour*, Technische Universiteit Eindhoven, Eindhoven **1999**.
- [13] L. Krüger, S. Wolf, S. Martin, U. Martin, A. Jahn, A. Weiß, P. R. Scheller, *Steel Res. Int.* **2011**, 82, 1.
- [14] B. Cao, T. Iwamoto, P. P. Bhattacharjee, *Mater. Sci. Eng. A* **2020**, 774, 1.
- [15] R. Eckner, L. Krüger, M. Motylenko, A. S. Savinykh, S. V. Razorenov, G. V. Garkushin, *DYMAT* **2011**, 183, 1087.
- [16] S. S. Hecker, M. G. Stout, K. P. Staudhammer, J. L. Smith, *Metal. Trans. A* **1982**, 13, 619.
- [17] T. Orsulova, P. Palcek, M. Roszak, M. Uhrick, M. Smetana, J. Kudelcik, *Proc. Struct. Integr.* **2018**, 13, 1689.
- [18] A. M. Beese, D. Mohr, *Exp. Mech.* **2011**, 51, 667.
- [19] B. Cao, T. Iwamoto, *Steel Res. Int.* **2017**, 88, 1700022.
- [20] C. Celada-Casero, H. Kooiker, M. Groen, J. Post, D. San-Martin, *Metals* **2017**, 7, 271.
- [21] T. Orsulova, P. Palcek, J. Kudelcik, *Prod. Eng. Arch.* **2017**, 14, 15.
- [22] S. H. Khan, F. Ali, A. N. Khan, M. A. Iqbal, *Comput. Mater. Sci.* **2008**, 43, 623.
- [23] M. Shirdel, H. Mirzadeh, M. H. Parsa, *Mater. Sci. Eng. A* **2015**, 624, 256.

- [24] D. Berger, A. Egloff, J. Summa, M. Schwarz, G. Lanza, H.-G. Herrmann, *Proc. CIRP* **2017**, 62, 39.
- [25] A. Devillez, D. Dudzinski, *Mech. Syst. Signal Proc.* **2007**, 21, 441.
- [26] G. Mroz, W. Reimche, FR.-W. Bach, *Cyber-Physical And Intelligent Systems In Manufacturing And Life Cycle*, Vol. 2, Academic Press, London, UK **2017**, p. 84.
- [27] P. Mayer, B. Kirsch, C. Müller, H. Hotz, R. Müller, S. Becker, E. V. Harbou, R. Skorupski, A. Boemke, M. Smaga, D. Eifler, T. Beck, J. C. Aurich, *CIRP J. Manufact. Sci. Technol.* **2018**, 23, 6.
- [28] B. Kirsch, S. Basten, H. Hasse, J. C. Aurich, *CIRP Annals* **2018**, 67, 95.
- [29] P. Mayer, B. Kirsch, R. Müller, S. Becker, E. V. Harbou, J. C. Aurich, *Proc. CIRP* **2016**, 45, 59.
- [30] F. C. N. Borges, P. R. Mei, L. P. Cardoso, J. Otubo, *Mater. Res.* **2008**, 11, 63.
- [31] P. C. Maxwell, A. Goldberg, J. C. Shyne, *Metall. Trans.* **1974**, 5, 1305.
- [32] G. Krauss, A. R. Marder, *Metall. Trans. A* **1971**, 2, 2343.
- [33] H. Schumann, *Kristall. Technik* **1975**, 10, 401.
- [34] G. B. Olsen, M. Cohen, *Metall. Trans. A* **1982**, 13, 1907.
- [35] A. Weiß, H. Gutte, J. Mola, *Metall. Trans. A* **2016**, 47, 112.
- [36] A. Stormvinter, P. Hedström, A. Borgenstam, *Solid State Phenom.* **2011**, 172–174, 61.
- [37] G. Krauss, *Mater. Sci. Eng. A* **1999**, 273–275, 40.
- [38] S. Morito, H. Yoshida, T. Maki, X. Huang, *Mater. Sci. Eng. A* **2006**, 438–440, 237.
- [39] L. V. Fricke, H. N. Nguyen, B. Breidenstein, B. Denkena, M.-A. Dittrich, D. Zaremba, H. J. Maier, *Techn. Messen*, Unpublished.
- [40] G. Faninger, U. Hartmann, *HTM* **1972**, 27, 233.
- [41] D. Stegemann, W. Reimche, K. L. Feiste, B. Heutling, *Nondestruct. Character. Mater.* **1998**, 269.
- [42] O. Bruchwald, W. Frackowiak, W. Reimche, H. J. Maier, *La Metall. Italiana* **2015**, 11/12, 29.
- [43] D. Mercier, J. Lesage, X. Decoopman, D. Chicot, *NDTE Int.* **2006**, 39, 652.
- [44] L. V. Fricke, M. G. Skalecki, S. Barton, H. Klümper-Westkamp, H.-W. Zoch, D. Zaremba, *HTM J. Heat Treatm. Mat.* **2019**, 74, 345.